PHYSICAL REVIEW A, VOLUME 64, 061402(R)

Relativistic laser-field-drift suppression of nonsequential multiple ionization

Matthias Dammasch,[1] Martin Dörr,[1,2] Ulli Eichmann,[1] Ernst Lenz,[1] and Wolfgang Sandner[1,2]
[1]*Max-Born-Institute for Nonlinear Optics and Short-Pulse Spectroscopy, 12489 Berlin, Germany*
[2]*Optisches Institut, Technische Universität Berlin, D-10623 Berlin, Germany*
(Received 12 April 2001; published 16 November 2001)

We have studied the multiple ionization of Xe with intense laser pulses. For the highest intensities, and, concomitantly, the highest ionic charge states, there is only evidence of sequential and not of simultaneous multiple ionization. The multiple-ionization rate below saturation is greatly reduced, compared to the theoretical predictions based on nonrelativistic multiple-ionization models. Since simultaneous multiple ionization requires the return of the first ionized electron to its parent atom, our results show suppression of this return. This suppression is expected to occur due to the relativistic photon momentum imparted by the laser field, as seen in simulations of relativistic classical trajectories.

DOI: 10.1103/PhysRevA.64.061402 PACS number(s): 32.80.Rm

Atomic ionization dynamics at laser intensities below 10^{16} W/cm^2 with laser pulses in the femtosecond regime has been extensively investigated over the past years (see, for example, [1]). A single active electron-tunneling formula describes very well the single electron ionization process [2]. The strong doubly and multiply charged ion yields measured for atomic systems in strong laser fields below the saturation intensity result from a nonsequential ionization process, which is by orders of magnitude larger than the sequential one [3]. The experimental data are fairly well understood in terms of a rescattering model [4], which provides an intuitive qualitative picture of the ionization mechanism: the first electron, set free by tunnel ionization under the influence of the external harmonic field, returns to the core to knock out the second electron. More recently, very detailed differential measurements on the momentum distribution of the ions [5] have been explained as well on the basis of this model [6].

At low laser intensity, and for laser wavelength long compared to the typical dimensions of the atomic system, one usually can use the dipole approximation in the description of the laser-atom interaction. This approximation amounts to neglecting the spatial variation of the laser field, and consequently its magnetic-field component plays no role.

The engineering of short pulse lasers with powers as high as 100 TW and intensities of over 10^{19} W/cm^2, allows for the study of ionization dynamics in a new regime [7–9]. When the particles are accelerated to relativistic speed, the magnetic-field component of the laser is no longer negligible, causing an average drift momentum of the photoelectron in the propagation direction. In the context of high-frequency adiabatic stabilization, this drift has been discussed in theoretical investigations to lead to the eventual suppression of stabilization at high laser intensities [10]. In the context of multiple ionization, this drift can lead to a reduced nonsequential ionization probability simply due to the fact that the rescattered electron misses the core. Similarly, in the context of harmonic generation [11], the harmonic yield is reduced due to the same reason. No measurements giving evidence of this relativistic suppression have been presented yet, to our knowledge, but there have been first ion yield measurements in Ar at relativistic laser intensities [9].

By observing the ejection angle of electrons obtained through ionization of Ne up to $8+$ and Kr up to $11+$, this drift has been measured [12]. It was seen that the electrons are ejected preferentially at an angle smaller than $90°$ with the laser propagation direction; this angle was smaller for larger ionic charge states and laser intensities. The results could be modeled quantitatively on the basis of simple classical trajectories.

In the present Rapid Communication, we give indirect evidence of this relativistic forward drift of the ionized electrons, by a measurement of the multiple-ionization yield for very high charge states of Xe at intensities well below saturation of the multiple ionization.

The measurements have been performed with laser light from the MBI high intensity laser facility. This light is guided through vacuum tubings into the target UHV chamber. The UHV vacuum chamber with a background pressure of about 5×10^{-9} mbar is separated from the beam guide vacuum tubings by a 0.5-mm thick quartz plate. The light beam, 5 cm in diameter, is focused by means of an f/2.8 off-axis parabola between two field plates, 1 cm apart. Multiply charged ions are extracted through an opening in one field plate by applying a constant electric field of a few hundred volts per centimeter. The ions are accelerated towards a multichannel plate detector and are mass and charge selected by their time of flight (TOF mass spectrometer). The spectrometer is operated in the ion counting mode. The atomic target is provided by filling the chamber with Xe gas to a given pressure. To reduce the detected effective interaction volume, we have the possibility to move a slit with a width of 0.3 mm over the opening in the field plate. The light exits the chamber through a glass port and is further analyzed with respect to pulse energy and pulse duration. The latter one is performed using a background free autocorrelator. Typical laser beam parameters are about 600-mJ pulse energy, 60-fs pulse duration, and an estimated focus spot size w_0 of 12 μm, which gives a maximum intensity of about 2×10^{18} W/cm^2 in the focus.

In Fig. 1 we show a TOF spectrum giving the different ionization stages of Xe at a pressure of 7×10^{-8} mbar after irradiation with a laser pulse of about 10^{18} W/cm^2. Data have been collected over 1024 shots. The spectrum has not been corrected for detection efficiency, which is expected to

 ©2001 The American Physical Society

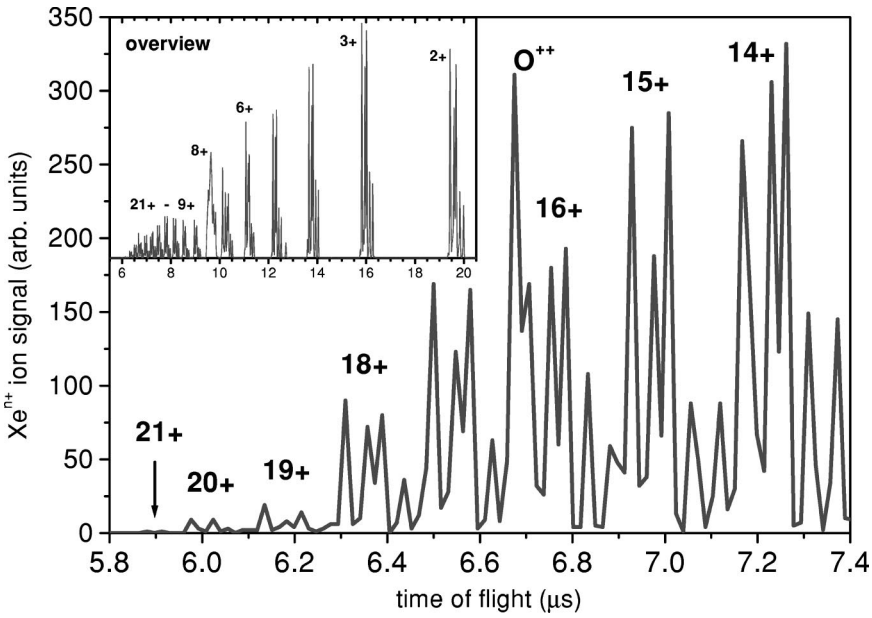

FIG. 1. Xe ion yield differentiated into charge states by TOF. The inset shows the complete spectrum, ranging from Xe^{2+} down to Xe^{21+}, leftmost.

change noticeably between highest and lowest charge states, but not significantly between the charge states 14 and 21. The five most abundant isotopes of Xe for each charge state are clearly resolved. Drops can be observed in the ion yields between the charge states 8 and 9, and between 18 and 19. These drops are due to electronic shell closing [13], namely main quantum number 5 at charge 8 and the 4d subshell at charge 18, causing a large increase in binding potential (see also Table I below). The highest charge state clearly visible in this spectrum is Xe^{20+}; the ion yield cuts off at Xe^{21+} and no Xe^{22+} is visible. From this we obtain immediately a rather accurate idea of the laser intensity, assuming that the laser intensity corresponds to the classical-field-ionization threshold of the highest observed charge state Xe^{20+}. By rule of thumb, ionization of a species bound with energy E in a Coulomb field of nuclear charge Z, appears around the critical (barrier suppression) field strength $F_C = E^2/4Z$ (in atomic units, a.u.). For ionization of Xe^{19+}, we obtain $F_C = 5.74$ a.u., corresponding to a laser intensity of 1.2×10^{18} W/cm^2. Consequently, the ion yield of Xe^{20+} is close to saturation, within the focal volume of highest intensities.

TABLE I. Ionization stages of Xe. E_{ion}: ionization energy to reach charge state, $n+$ from the initial charge state $(n-1)+$. $F_C = E_{ion}^2/4Z$, where $Z=n$: critical field for this ionization (namely from charge stage $n-1$ to n). $\Delta p = 2/a = E_{ion}^{3/4}/\sqrt{2^{1/2}Z}$: momentum width of the resulting ionized wave packet. p_i: transverse initial momentum leading to a trajectory returning to the origin, for start phase 9 °.

$n+$	E_{ion}	F_C	Δp	$-p_i$
15	13.2	2.88	1.50	4.3
16	14.3	3.21	1.55	5.3
17	15.5	3.52	1.59	6.2
18	16.6	3.83	1.63	7.3
19	20.2	5.36	1.84	13.3
20	21.4	5.74	1.87	14.9
21	22.7	6.14	1.91	16.8

In Fig. 2 we compare the integral ionic charge state yields with the results from two different theoretical calculations. For these calculations, we solve rate equations connecting the various charge states. The laser pulse duration and the intensity distribution in the focused laser beam are taken into account [14]. In the calculations, the single electron ionization rates for the processes $Xe^{n+} \rightarrow Xe^{(n+1)+}$ are estimated using the Ammosov-Delone-Krainov (ADK) tunneling formula [2]. The results labeled ''sequential'' are computed using only these rates. The ''simultaneous'' results include additionally nonsequential rates. As a simple approximation,

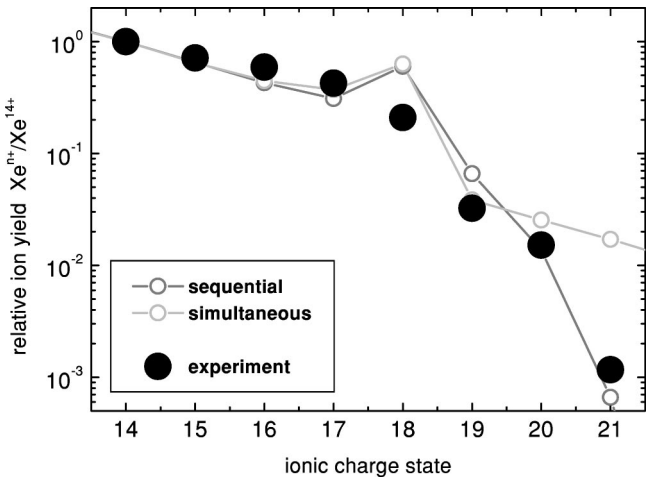

FIG. 2. Multiply charged ion yield for Xe at a laser intensity of about 10^{18} W/cm^2. The solid black circles give the experimental results (the uncertainty in y direction is smaller than the circle radius, even for the 21+ result). The lighter circles connected by lines give the results from numerical simulations using rate equations, at peak intensity 1.57×10^{18} W/cm^2. The ''simultaneous'' results include nonsequential multiple-ionization rates, the ''sequential'' ones do not.

we have chosen an empirical formula [14,15], which has been found to be valid over a wide range of intensities for charge states up to Xe^{10+} [16]. We do not require a high accuracy of the formula: the only requirement is that the nonsequential probability strongly exceeds the sequential one for charge states whose ionization is not saturated. The experimental points are normalized to the theoretical Xe^{14+} yield, set arbitrarily to 1. All three sets of results are in good agreement up to and including charge state 20. An exception is state 18, for which the calculation overestimates the experimental result: the enhancement is due to the 4d shell closing (see above), and the discrepancy may originate in an inadequacy of the ADK rates used [17], which manifests particularly for closed shell ionization.

That there is hardly any difference between the ''sequential'' and the ''simultaneous'' results is simply due to saturation: the dramatic difference between the two multiple ionization pathways (usually several orders of magnitude) is only apparent when the lower charge state is not completely ionized [3]. Thus, the additional simultaneous rates enhance the yields of Xe^{20+} and Xe^{21+}, and consequently reduce slightly the final yield of Xe^{19+}. Our principal result, however, is the one for the highest charge state, Xe^{21+}. Here, the experimental results clearly point towards the sequential rather than the simultaneous results, indicating the suppression of nonsequential multiple ionization.

In order to quantify relativistic effects, we perform a classical relativistic trajectory calculation for the ionized electrons in the combined presence of the laser field and the Coulombic field of the core. Consider an electron set free by tunnel ionization at time $t=t_0$ and at position $x=x_0$, $y=y_0$, $z=z_0$ with initial velocity v_{x0}, v_{y0}, v_{z0}. It is then accelerated by a plane-wave harmonic laser field with y-component vector potential $A(x,t)=A_0\sin(\omega(t-x/c)-\phi)$, so that the electric field is $E(x,t)=E_0\cos(\omega(t-x/c)-\phi)$. The wave is polarized in the y direction and the propagation of the field is in x direction. Furthermore, we also include a static Coulomb potential, with charge Z. It turns out that for the Xe^{20+} results, the Coulomb potential refocusing [18] plays no important role since we consider only the first return. Typical trajectories are depicted in Fig. 3. The quantum-mechanical wave packet released by the field from the atom has a position width and concomitant momentum spread, and we model the initial conditions by a corresponding classical ensemble.

The initial distribution of positions and momenta of the wave packet is determined by tunneling [2,18,19]. Thus, we choose y_0 around the end of the classical tunnel, $y_0=y_T=|E|/F$ and x_0 around 0. The spatial $1/e$-half-width a in direction transversal to the E-field direction of the probability flux emerging around the end of the classical tunnel is given by $a^2=\hbar^2k/(mF)$. Here $\hbar$ and m are the usual quantities ($=1$ in a.u.), F is the (static) field strength, and $k=\sqrt{2m|E|}/\hbar$, with E the (unshifted) binding energy. The momentum distribution in the transverse direction is the (2D) Fourier transform of the spatial wave function, and therefore half of the $1/e$ width in transverse momentum is equal to $1/a$. It is this transverse momentum spread that leads to the spreading of the wave packet, during its excursion.

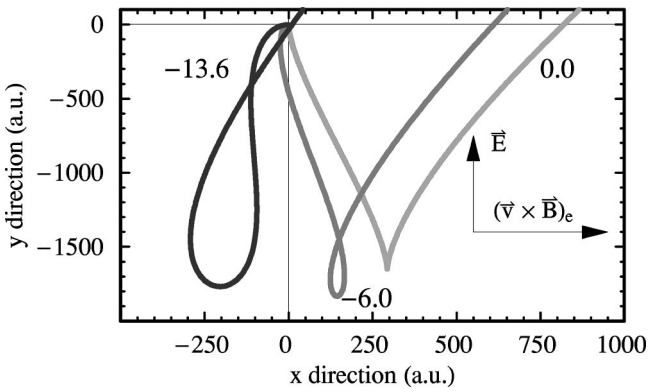

FIG. 3. Representative classical relativistic trajectories for an electron in the field of a Xe^{20+} nucleus ($Z=20$) and a plane-wave field of peak strength $F=5.7$ a.u. (intensity 1.2×10^{18} W/cm^2), wavelength 800 nm. The initial position is $(x,y)=(0,-2)$ and the initial velocity is $v_y=0$ and v_x given by the numbers next to the trajectories. The trajectories are shown over approximately half a period of the laser field and the initial time t_0 is such that the particle is set free at a phase of the field $\phi=18°$.

In accord with the rescattering model [4,18], we then calculate the fraction of electrons from this initial ensemble that returns close to the core, within a given radius r_0, in order to strongly interact with one of the remaining electrons to cause double ionization, within one field period. The radius r_0 is determined by the typical binding radius of the outer core electrons and, to a lesser extent, by the energy-dependent e-2e scattering cross section [20]. This leads to a range of initial conditions, x_0, y_0, z_0, v_{x0}, v_{y0}, v_{z0}, all depending on the initial time t_0 (or the corresponding initial phase ϕ of the laser field). Just as for the nonrelativistic case, if $v_{y0}=0$, only trajectories with initial time such that the field phase at t_0 is between $0<\phi<\pi/2$ can return to the core. Since the radius r_0 is very small, the range of initial conditions that allows return is very narrow. The results from the trajectory calculation for an electron ionized from Xe^{19+} are depicted in Fig. 4.

Since the field strength at t_0 determines the first electron's tunnel ionization probability, this cuts off the allowed initial times exponentially around approximately 30°. Since the particle must return to the origin with sufficient energy, the return energy (not shown) suppresses the probabilities close to phase 0. The main point is now that the starting momentum in direction opposite to the laser propagation direction must be between 1 and 0.4 times its peak value over the range of start times allowed. The peak value of this initial momentum, required to balance the relativistically induced drift momentum, is 17.7 a.u. for the case of Xe^{19+} considered in Fig. 4. The momentum width of the initial electronic wave packet set free from Xe^{19+} is, however, $1/a=[(21.4)^{1/2}/5.7]^{(-1/2)}=0.94$ a.u. Comparing with the results of Fig. 4, we find that the required initial momentum for the electron to return close to the core is about a factor of 10 larger than the $1/e$-half-width of the momentum distribution. Thus the return probability is suppressed by several orders of magnitude compared to a nonrelativistic calculation without the magnetic-field drift.

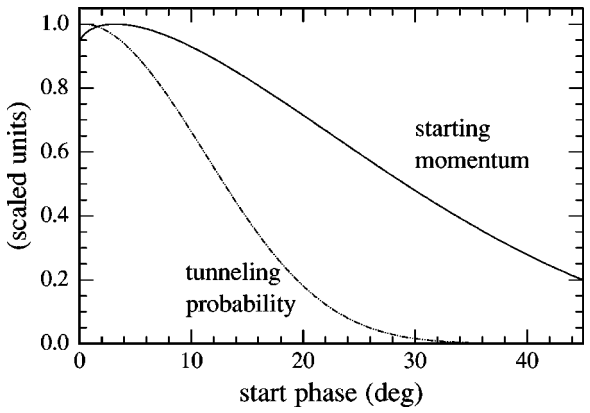

FIG. 4. Classical trajectory calculation results for ionization $Xe^{19+} \rightarrow Xe^{20+}$ and return to the Xe^{20+} core. Solid line: required initial momentum $-mv_{y0}$ in the field propagation direction, as a function of the initial phase of the field at ionization time t_0. Dashed line: tunnel ionization probability. The curves have been scaled to 1 at their peak values.

Table I gives an overview of the typical parameters for Xe^{n+} charge states from $n=15$ to $n=21$. For each charge state, the ionization energy from the previous $(n-1)$ charge state is given, together with its critical field strength and the resulting tunnel ionized wave packet's tranverse momentum spread. The momentum required to balance the relativistic drift is given as p_i, computed for start time at phase 9° of the field, giving 95% of the maximum momentum, as shown in Fig. 4. Due to the different scaling of Δp and $-p_i$ with n, the shell jump from $n=18$ to $n=19$ boosts their ratio by almost a factor of two, making the relativistic suppression of return probability apparent. It must be noted that the velocity of the electron at the field strengths presented here never becomes strongly relativistic, staying below 0.75 °C. The drift effect is a consequence of the magnetic component of the laser field.

Concluding, we have obtained indirect evidence for the suppression of nonsequential multiple ionization in very intense laser fields. This suppression appears for (i) sufficiently intense fields and (ii) sufficiently highly charged ionic species. The highly charged ions can survive to experience the high laser fields and their ionization must be well below the saturation in order to exhibit the nonsequential ionization effects. In our case, this has been observed in the ionization yield of Xe for the charge state 21+. In fact, it is hard to disentangle this relativistic drift suppression from other factors such as change in ionization rates with laser intensity or ionic charge state. In order to observe the reduction in nonsequential multiple ionization, it is important to measure the ion yields at laser intensities below saturation of the ionization. The suppression of nonsequential ionization is interpreted in terms of the relativistic drift acquired by the ionized electrons from the laser. Further experiments will be performed to extend the data to a range of intensities and further charge states.

We are grateful to Wilhelm Becker for helpful discussions and we thank M. Kalashnikov and V. Karpov for running the laser system. This work was supported by the Deutsche Forschungsgemeinschaft.

[1] *Multiphoton Processes*, edited by L. F. Mauro, R. R. Freeman, and K. C. Kulander, AIP Conf. Proc. No. 525 (AIP, New York, 2000).

[2] M.V. Ammosov, N.B. Delone, and V.P. Krainov, Zh. Éksp. Teor. Fiz. **91**, 2008 (1986) [Sov. Phys. JETP **64**, 1191 (1986)].

[3] B. Walker, B. Sheehy, L.F. DiMauro, P. Agostini, K.J. Schafer, and K.C. Kulander, Phys. Rev. Lett. **73**, 1227 (1994).

[4] P.B. Corkum, Phys. Rev. Lett. **71**, 1994 (1993).

[5] Th. Weber *et al.*, Phys. Rev. Lett. **84**, 443 (2000); R. Moshammer *et al.*, *ibid.* **84**, 447 (2000).

[6] R. Kopold, W. Becker, H. Rottke, and W. Sandner, Phys. Rev. Lett. **85**, 3781 (2000).

[7] K. Yamakawa, M. Aoyama, S. Matsuoka, T. Kase, Y. Akahane, and H. Takuma, Opt. Lett. **23**, 1468 (1998).

[8] B.C. Walker *et al.*, Opt. Express **5**, 196 (1999).

[9] B.C. Walker, E.A. Chowdury, C. Toth, K.R. Wilson, and C. P.J. Barty, in Ref. [1], p. 667 (2000); E.A. Chowdhury, C.P.J. Barty, and B.C. Walker, Phys. Rev. A **63**, 042712 (2001).

[10] N.J. Kylstra, R.A. Worthington, A. Patel, P.L. Knight, J.R. Vazquez de Aldana, and L. Roso, Phys. Rev. Lett. **85**, 1835 (2000); J.R. Vazquez de Aldana and L. Roso, Opt. Express **5**, 144 (1999); T. Katsouleas and W.B. Mori, Phys. Rev. Lett. **70**, 1561 (1993).

[11] D.B. Milosevic, S. Hu, and W. Becker, Phys. Rev. A **63**, 011403(R) (2001); M.W. Walser, C.H. Keitel, A. Scrinzi, and T. Brabec, Phys. Rev. Lett. **85**, 5082 (2000); N.J. Kylstra, R.M. Potvliege, and C.J. Joachain, J. Phys. B **34**, L55 (2001).

[12] C.I. Moore, J.P. Knauer, and D.D. Meyerhofer, Phys. Rev. Lett. **74**, 2439 (1995); D.D. Meyerhofer, J.P. Knauer, S.J. McNaught, and C.I. Moore, J. Opt. Soc. Am. B **13**, 113 (1996); S.J. McNaught, J.P. Knauer, and D.D. Meyerhofer, Phys. Rev. Lett. **78**, 626 (1997); Phys. Rev. A **58**, 1399 (1999).

[13] S. Augst, D. Strickland, D.D. Meyerhofer, S.L. Chin, and J.H. Eberly, Phys. Rev. Lett. **63**, 2212 (1989).

[14] H. Maeda, M. Dammasch, U. Eichmann, and W. Sandner, Phys. Rev. A **63**, 025401 (2001).

[15] U. Eichmann, M. Dörr, M. Maeda, W. Becker, and W. Sandner, Phys. Rev. Lett. **84**, 3550 (2000).

[16] M. Dammasch, Ph.D. thesis, Technical University of Berlin, 2001.

[17] R. Taieb, V. Veniard, and A. Maquet, Phys. Rev. Lett. **87**, 053002 (2001).

[18] G.L. Yudin and M.Yu. Ivanov, Phys. Rev. A **63**, 033404 (2001); H.W. van der Hart and K. Burnett, *ibid.* **62**, 013407 (2000).

[19] B. Gottlieb, A. Lohr, W. Becker, and M. Kleber, Phys. Rev. A **54**, R1022 (1996).

[20] V.A. Bernshtam, Yu.V. Ralchenko, and Y. Maron, J. Phys. B **33**, 5025 (2000).